11th International Conference on Contact Mechanics and Wear of Rail/Wheel Systems (CM2018), Delft, The Netherlands, September 24-27, 2018

QUANTIFYING ROLLING CONTACT FATIGUE IN RAILS

Daniel Szablewski [1], Alok Jahagirdar [1]
[1] National Research Council (NRC) Canada, Automotive and Surface Transportation (AST), Ottawa, Canada

E-mail: daniel.szablewski@nrc-cnrc.gc.ca, alok.jahagirdar@nrc-cnrc.gc.ca

Abstract: Accurate quantification of Rolling Contact Fatigue (RCF) cracks in a broad range of rail steels remains elusive due mostly to the complexity of analysis required to map the RCF occurrence in rails utilized in a variety of track and loading conditions. Presented work proposes a way forward to map RCF cracks based on their position on the railhead, their depth, length and angle to the running surface. Results for five (5) rail steels are shown in detail. In addition, the plastic deformation layer in these rail steels is assessed by both light optical microscopy and microhardness techniques.

Keywords: rail, wear, rolling contact fatigue, crack morphology, plastic deformation, RCF matrix, rail maintenance, eddy current

1. Introduction

Wear and rolling contact fatigue (RCF) in premium and intermediate hardness rail steels has been investigated in the recent past [1-10]. These investigations considered wear and RCF performance in 20 different rail steel types utilized in a ~35-tonne/axle heavy axle load (HAL) train environment in a 349-meter (m) radius curve, with as much as 500 million gross tons (MGT) accumulation on the rails over their life-cycle in track [1-8], as well as twin disk testing [9,10]. Recent investigations on rail steels point to a number of relevant observations:

- RCF is the dominant mode of failure in premium rail steels, as the RCF growth rate in premium rails outpaces rail wear rate. [2,4,5,7,8]
- An increase in premium rail hardness is achieved primarily through an increase in carbon content. However, rails with hyper-eutectoid carbon compositions are prone to occurrence of grain boundary cementite (Fe_3C) phase, which has detrimental influence on RCF formation and propagation in rail steels. [1,4,5,7]
- In hypoeutectoid steels RCF initiation was observed at highly strained grain boundary pro-eutectoid ferrite phase. [12,13]
- There is a poor relationship between carbon content in premium rail steels and the respective rail hardness. This is attributed to the influence of thermo-mechanical rail processing during rail production and its significant influence on the rail microstructure. [4,5,7]
- Decarburization in rail steels at the running surface decreases the rail running surface hardness, while increasing the wear rate and RCF crack growth rate. [9,10]
- Current RCF assessment methods on the rail head running surface are mostly qualitative (i.e. visual, dye penetrant based or magnetic particle based) or semi-quantitative (i.e. machine vision systems), where image acquisition and its rating is done automatically by a machine, effectively removing the user influence on the results. However, quantitative methods (i.e. eddy current) are gaining an interest in the railroad community as these methods offer a numerical assessment of RCF and are user independent. [8,11]
- Initial investigations suggest that eddy current (EC) and magnetic flux inspection methods have the potential to accurately measure RCF depth in the rail. More work needs to be done to verify calibration and accuracy of these methods. [11]

Considering these past results, the next step in RCF research would be to develop growth rate prediction models as a function of rail position in the curve and accumulated tonnage in the rail life-cycle. This could be achieved through detailed investigation of RCF morphologies in rails at variable points in their life-cycle. Quantitative RCF results from such investigation would be placed in an 'RCF Matrix'.

2. Development of an 'RCF Matrix'

RCF morphology can be subdivided into quantitative features to identify the important aspects of the crack, such as: position on the railhead, length, depth, angle to running surface, and amount of branching. These RCF morphological features are largely dependent on how the rail is utilized in track (i.e. what track curvature the rail is placed in, and what the tonnage accumulation is on the rail). Past RCF investigations of worn premium rails that have been utilized in a high rail position [7,8] have shown that RCF angle is shallow on the lower gage face corner (GFC) and becomes more steep as the position shifts to the top-of-rail (TOR) running surface (Figure 1).

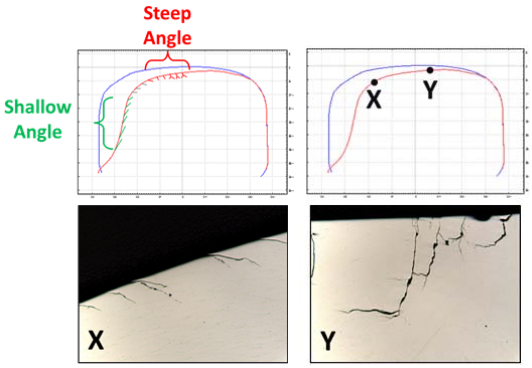

Figure. 1 Typical high rail RCF crack morphology for rail utilized in HAL traffic environment. [8]

A detailed analysis of the depth and angle features of RCF cracks in three different rail grades (with varying amounts of carbon content) that originated from the same operating track environment, revealed that crack depth is a function of the rail grade utilized in service. In other words, in this RCF study cracks propagated faster in rails with higher carbon content. However, all investigated rails had a similar distribution of crack angles to the running surface (Figure 2). This suggests that RCF crack angle is a function of wheel/rail contact and train operating conditions, rather than rail type utilized in track.

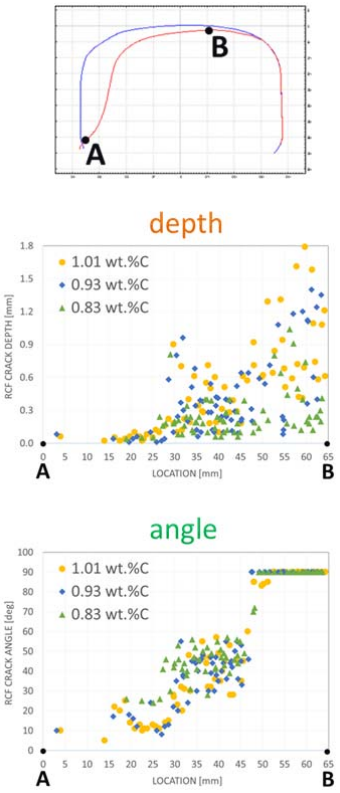

Figure. 2 RCF crack depth and angle for three rail grades with varying carbon contents. [8]

The study presented above was done on a limited number of rail steels placed in one specific track location. To better understand the behavior of RCF on a global scale more analysis layers need to be considered. These include the following:

- rail grade (i.e. standard, intermediate, premium)
- track curvature (i.e. variable radius)
- tonnage accumulation (i.e. MGT)
- running surface condition (i.e. dry, lubricated, TOR friction modified)
- traffic type (i.e. axle load, train speed)
- maintenance grinding (frequency and amount)

In addition, the way in which RCF is investigated needs to be methodical in approach to allow accurate comparison of results across multiple layers. This is a massive undertaking that will require a great deal of resources, some of which were outlined in recent presentations [14,15].

The acquired RCF morphology quantitative results can be placed in a matrix to develop RCF growth rate models for specific set of track conditions. The number of layers present in this matrix (some of which were outlined above) means that the matrix would be multi-dimensional. The information would be accessible in a 2-dimensional format depending on the layers of interest under consideration.

3. Investigation of 5 Rail Types

The results presented in this paper outline RCF metrics for five (5) rail types across 5 different curvatures and MGT levels (see Table 1). This investigation serves as an outline of a methodical approach to RCF crack analysis in rail steels.

Table 1: Rail curvature, approximate accumulated MGT, origin, and type for 5 rails investigated.

Sample #	Curvature [deg]/[m radius]	Approx. Accum. [MGT]/m-tonne	Rail Origin	Rail Type
1	0 / tangent	1050 / 953	CN Superior (MP T368.6)	Algoma-Canada CC 115 RE (1980)
2	1.0 / 1747	750 / 680	NS Hardy	136 RE (1990)
3	2.0 / 873	630 / 572	BNSF Staples (MP 200.69)	136 RE (1994)
4	4.45 / 392	570 / 517	CN Superior (MP 417.3H)	Beth Steelton 136 RE (1997)
5	4.75 / 368	570 / 517	CN Superior (MP 467.23)	Beth Steelton 136 RE (1997)

The rails range from tangent to 368 m-radius curve track. All rails investigated (except for tangent track) were from the high rail location, and were taken out of service following regular rail replacement. As a result, accumulated MGT for each rail is a reflection of in-service life-cycle for that specific rail at the utilized track location. This explains the decrease in accumulated MGT as the track curvature increases, as high rails utilized in higher curvatures reach the gage face wear limit(s) (depending on railroad operating practice) faster than high rails at lower curvatures.

Rail acquisition for metallography and RCF investigation remains a highly opportunistic endeavour, as rails with remaining wear life-cycle are usually not removed from service prematurely. As a result, this type of study acquires rails with variable MGT from variable curvatures. A challenge that can only be overcome by collecting large volumes of samples, with the targeted aim of acquiring a distribution of MGT at fixed curvatures, which in turn would allow a direct MGT comparison of RCF metrics (as described in this paper) across variable curvatures.

A collection of large volumes of samples remains the primary goal of this type of investigation, and this goal will be pursued in the near future. For now, presented results are for the 5 rail types addressed in Table 1.

4. Sample Sectioning

The rail samples (except the tangent) were cut at two locations: 90° and 45° cut planes, as indicated in Figure 3. The tangent was only cut at a 90° plane. Since the RCF is closely related to the longitudinal wheel creep and subsequently to wheel angle-of-attack (AoA) in relation to the rail running surface [16] the cracks

initiate at an angle to the rail longitudinal direction, as indicated in Figure 3. As a result, the selected cut planes for RCF analysis are aimed at capturing two slices of the 3-dimensional crack planes to understand the crack metrics (i.e. length, depth and angle) in relation to position on the railhead.

When considering visible RCF cracks on the running surface in a selected rail type the 90° cut plane yields less RCF cracks than the 45° cut plane. This is due to the fact that spacing between subsequent RCF cracks in a 90° cut direction (ΔL_1) is greater than RCF spacing in a 45° cut plane (ΔL_2). This becomes more apparent when viewing RCF results presented in Figure 5.

Since the 45° cut plane covers a greater distance than does a 90° cut plane, the RCF position on the railhead needs to be related to the vertical cut plane to allow a direct comparison of RCF position between the two cuts. To that end, a vertical component of the RCF position on the railhead (f_y=Lcosθ) was taken for all the crack position in the 45° cut plane (as indicated in Figure 3).

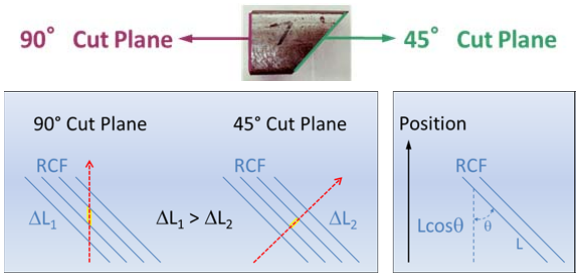

Figure 3. TOR view indicating the orientation of 90° and 45° cut planes as they relate to RCF visible on the rail surface. Calculation of position component (f_y) for 45° cut plane is also indicated.

5. Sample Metallography

A comparison of the RCF morphology in 90° cut planes revealed that RCF in tangent track tends to produce long shallow cracks that extend quite some distance into the bulk structure of the rail (see Sample #1 in Figure 4). The deformation that is accompanying these cracks is confined to layers between these cracks, as evidenced by the nital etched micrograph. Grain boundaries in deformed layers are indistinguishable, however the flow pattern of these deformed grains is quite clear and coincides with the plastic deformation of the rail running surface due to lateral creep forces [16]. The microstructure of the bulk rail is undeformed however, and the grain pattern is clearly evident in that structure.

At higher curvatures (368 m-radius in Sample #4) the wheel flanging on the gage side of the rail introduces a substantial amount of localized downward metal shear in the rail. This deforms the microstructure (with metal flowlines running downwards at shallow angles, as shown in Sample #4 etched micrograph), though the bulk of the microstructure is also undeformed. Visual observation of crack angle as a function of position on the rail cross-section indicates a shallow to steep progression where gauge face RCF cracks are primarily in the 10-20° angle range, and TOR RCF cracks are primarily in the 70-90° range.

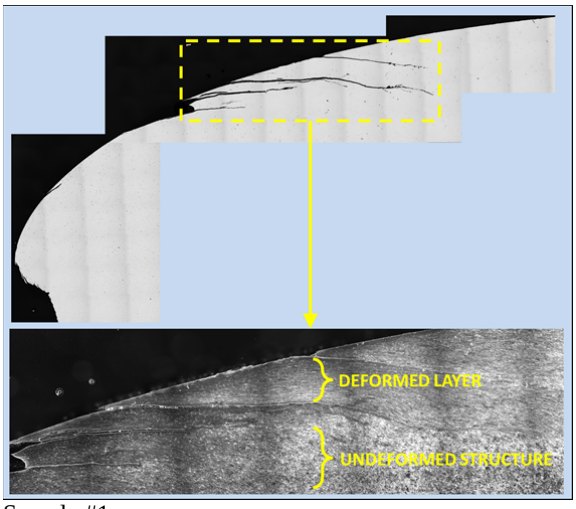

Sample #1

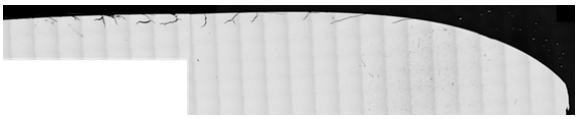

Sample #2

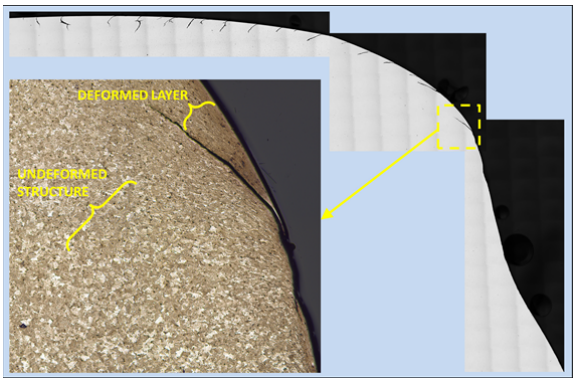

Sample #4

Figure 4. 90° cut plane mosaics of Sample #1, 2, and 4 indicating cross-sectional differences in RCF morphology along with the deformed layer (as evidenced by the 4% nital etched samples viewed under dark field (sample #1) and bright field (sample #4) conditions).

These observations hold true for intermediate curvatures as well (see Sample #2 in Figure 4), which goes to show that wheel flanging (causing top to bottom creep in rail structure) and wheel tread (causing lateral creep in rail structure) have a high degree of influence on the microstructure deformation in rail steel at the running surface. This in turn causes RCF crack initiation and propagation in these local structures.

6. RCF Quantitative Analysis

Measurements of the RCF cracks in the investigated rail steels were carried out for crack length, depth and angle at 90° and 45° cut planes. Measurement results as a function of position on the rail running surface (with 0 mm representing the gauge face corner of the high rail, and 100 mm the TOR running surface location) are

presented in Figure 5. The 45° cut plane for sample #1 was not be obtained.

90° Cut Plane

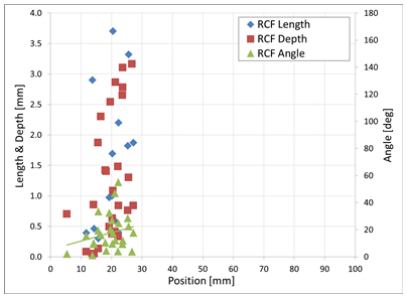

Sample #1

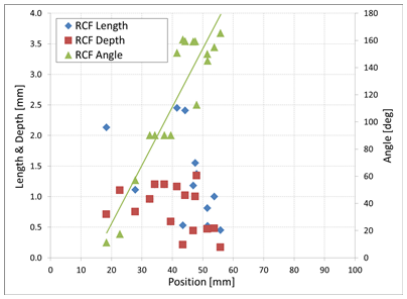

Sample #2

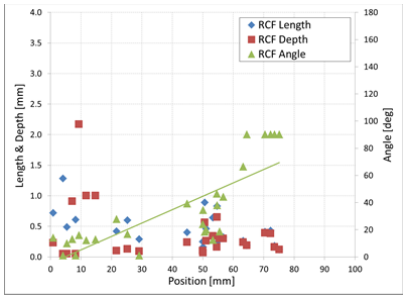

Sample #3

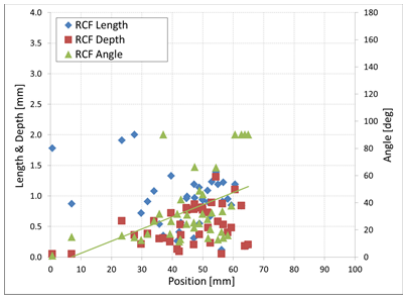

Sample #4

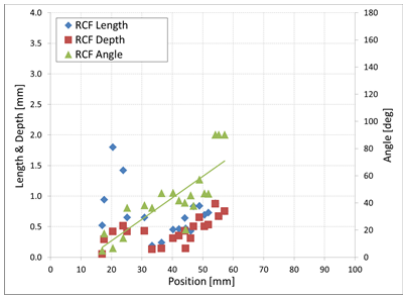

Sample #5

RCF cracks in tangent rail (sample #1) were observed on a relatively narrow band of the running surface close to the gauge face corner of the rail (see Figures 4 and 5). The angle range of RCF cracks in these rails was also relatively shallow (average 10-25° range, with select cracks reaching up to 40-50° range). The rise in RCF crack angles with increasing position was more substantial at higher degree curvatures. The highest angle rise was observed in sample #2.

The 45° cut plane intersected a greater number of cracks (with the shortest distance between them due to the perpendicular orientation of the observed plane to crack initiation surface witness marks). As a result, the density of cracks in the 45° cut plane was greater than that in the 90° cut plane, as evidenced in the results.

In samples #2 and #3 the depth measurements appeared greater in the 45° cut plane, indicating that the 90° cut plane most likely did not catch the dominant growth direction of the cracks.

45° Cut Plane

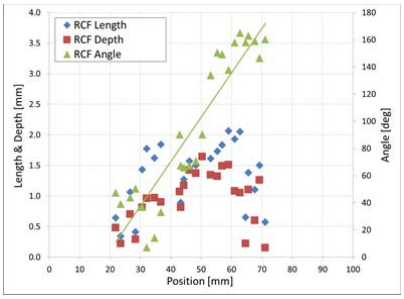

Sample #2

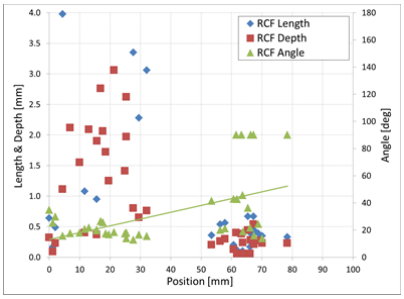

Sample #3

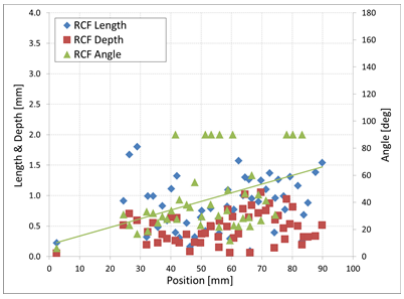

Sample #4

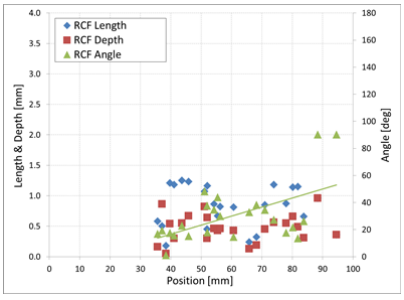

Sample #5

Figure 5. RCF measured Length, Depth and Angle as a function of position on the railhead for 90° and 45° cut planes.

However, in other rail types (samples #4 and #5) the measured depth of cracks appeared relatively unchanged indicating that dominant crack growth direction was approximately mid-way through the taken cut planes.

Definite trends in the crack depths and lengths could not be established with the limited available number of rail samples. As a result, acquisition of these trends will be postponed until more rails with RCF cracks are collected and analysed by presented methodology.

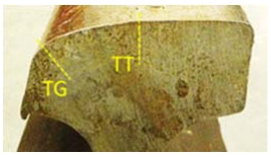

TT: Transverse Top-of-Rail (TOR)
TG: Transverse Gauge

TG Microhardness Traces

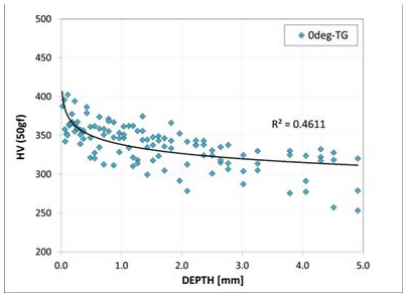

Sample #1

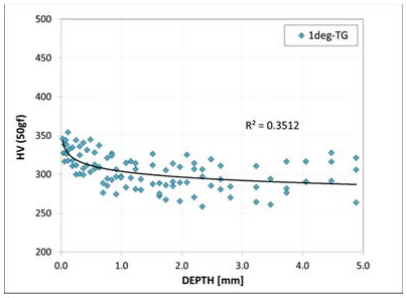

Sample #2

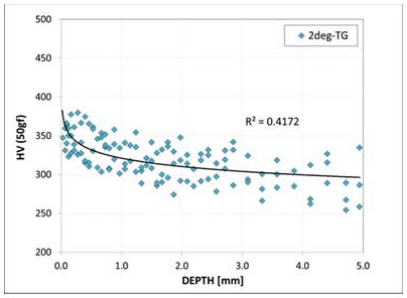

Sample #3

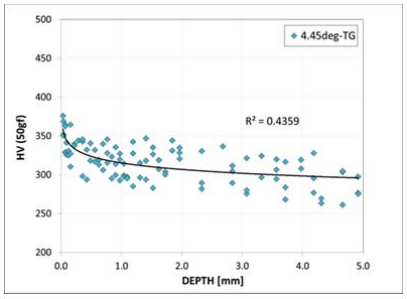

Sample #4

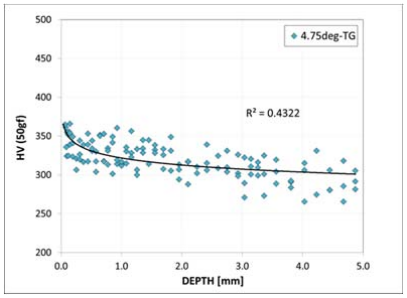

Sample #5

TT Microhardness Traces

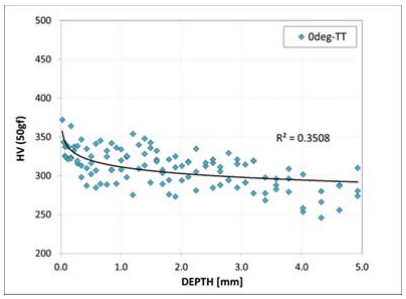

Sample #1

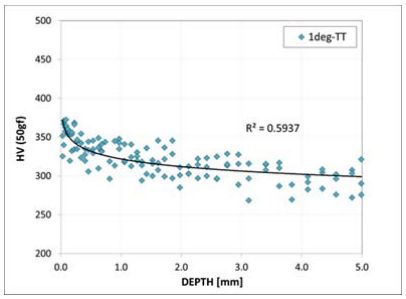

Sample #2

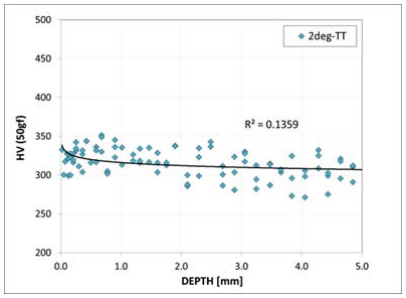

Sample #3

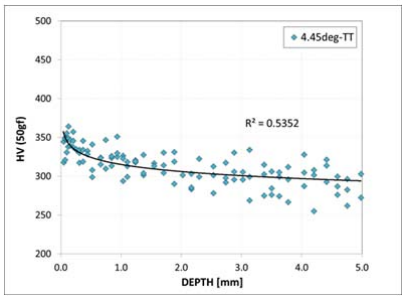

Sample #4

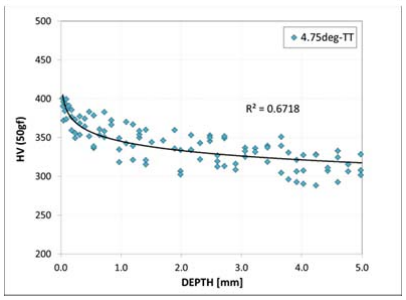

Sample #5

Figure 6. Vickers (50gf) microhardness traces for Transverse Gauge (TG) and Transverse Top-of-Rail (TT) locations.

7. Microhardness Analysis

Microhardness assessment in the investigated rail steels was carried out at two locations: the Transverse TOR and Transverse Gauge, TT and TG respectively (see Figure 6). 50gf load was utilized with a Vickers indenter to ensure a high density of measurements in the localized deformed layer of each rail type's TT and TG locations. Indent size and depth to running surface measurements were carried out on a light optical microscope at X500 magnification to guarantee a high degree of accuracy in data sets.

In all the measured profiles the deformed layer extended to approximate maximum depth of 2mm, with the bulk rail hardness stabilizing the hardness measurements past that depth. Average bulk hardness for all rail types was in the 290-320HV range, whereas the peak deformed layer hardness was in the 350-400HV range. The TG traces indicated more deformation in rail samples #1, 3, and 4, and TT traces in rail samples #2 and 5. However, the most obvious difference occurred in sample #1, whereas other samples showed relatively smaller hardness differences between the two locations.

For tangent rail (sample #1) this suggests that excessive plastic deformation at the TG location leads to a higher hardness zone near the running surface, which in turn leads to RCF formation at that location (see Figures 4-6). For other rail types the plastic flow layer (evidenced by microhardness measurements) is more even on the rail running surface, meaning that wheel contact on these rails is most likely conformal. This leads to RCF distribution over a wider range of rail contact surface (as show in Figure 5).

Presented results highlight the influence of plastic metal flow on RCF crack initiation and propagation. More rails are needed to build stronger trends in the collected data.

8. Conclusions

This paper outlined a systematic approach to analysing RCF cracks in revenue service rails. Focus was on measuring crack length, depth and angle as a function of position on the rail running surface, and then to relate these results to plastic metal flow measured by microhardness tests and observed through sample metallography techniques.

Results indicate that in tangent rail (sample #1) high degree of plastic deformation at TG location leads to a high hardness zone, which in turn leads to localized RCF occurrence (see Figure 4-6). Other rails however indicate a more uniform RCF crack distribution, which is supported by a more uniform plastic zone distribution, evidenced by the close proximity of TG and TT microhardness traces. This suggests that wheel/rail contact in these rails is most likely conformal.

The main aim of this work was to provide a systematic approach to analysing RCF cracks. This goal was achieved with the 5 analysed rails at various track curvatures and MGT accumulated levels. However, greater usefulness of this data will be realized by systematically organizing the results into an RCF matrix, accessible through a variety of input layers described in section 2 of this paper. To achieve that however, more rails with RCF are needed for analysis.

Placing the presented results into an RCF matrix will allow a comprehensive documentation of RCF features in service rails. This approach will permit easy access of RCF metrics by on-track maintenance personnel to facilitate the optimization of grinding schedules. It will also grant access of data to RCF modelling experts to facilitate more accurate forecasting of RCF growth in tracks under varying operating conditions. Both of these end user groups will benefit from the acquired information to facilitate the extension of rail life-cycles.

In addition, accurate prediction of RCF behaviour in service rails is critical to enable safe train operating practices. The presented results aim at accomplishing that goal.

9. Future Work

NRC continues to acquire rails with variable amounts of RCF for analysis of crack morphologies. The main idea behind this is to continue populating the RCF matrix for variable rail placement, loading, and other in-service operating conditions. Analysis of greater volume of rails is needed to build robust trends in the results. As these become available they will be reported to the railroad community at large.

10. Acknowledgements

This research was made possible through funding by the U.S. Department of Transportation Federal Railroad Administration (FRA) grant to the National Research Council (NRC) Canada.

References

[1] R. Ordóñez Olivares, A. J. DeArdo, C. I. Garcia, D. Szablewski, *New Rail Steel for the 21st Century: Advanced Alloy Thermo-Mechanical Processing Development*, Technology Digest, TD-09-011, Association of American Railroads (AAR) / Transportation Technology Center, Inc. (TTCI), Pueblo, Colorado, April 2009

[2] D. Szablewski, S. Kalay, J. LoPresti, *Preliminary Evaluation of Premium Rail Steels for Heavy Haul Operations*, Technology Digest, TD-11-031, Association of American Railroads (AAR) / Transportation Technology Center, Inc. (TTCI), Pueblo, Colorado, September 2011

[3] D. Szablewski, S. Kalay, J. LoPresti, *Preliminary Evaluation of Intermediate Hardness Rails for Heavy Haul Operations*, Technology Digest, TD-11-032, Association of American Railroads (AAR) / Transportation Technology Center, Inc. (TTCI), Pueblo, Colorado, September 2011

[4] D. Szablewski, J. LoPresti, D. Sammon, *Premium Rail Testing at FAST*, Technology Digest, TD-13-016, Association of American Railroads (AAR) / Transportation Technology Center, Inc. (TTCI), Pueblo, Colorado, July 2013

[5] D. Szablewski, S. Kalay, J. LoPresti, *Development and Evaluation of High Performance Rail Steels for Heavy Haul Operations*, International Heavy Haul Association (IHHA) Conference, 2011, Calgary, Canada

[6] D. Szablewski, J. LoPresti, *Intermediate Strength Rail Testing at FAST: Wear, RCF, and Deep-Seated*

Shelling Analysis, TD-14-010, Association of American Railroads (AAR) / Transportation Technology Center, Inc. (TTCI), Pueblo, Colorado, May 2014

[7] D. Szablewski, J. LoPresti, *FAST Premium Rail Test Results: 2010 through 2013 Test Period*, TD-14-021, Association of American Railroads (AAR) / Transportation Technology Center, Inc. (TTCI), Pueblo, Colorado, October 2014

[8] D. Szablewski, *FAST Sec. 7 Premium Rail Test Results*, TTCI Annual Review poster presentation, 2013

[9] R.I. Carroll, J.H. Beynon, *Decarburisation and Rolling Contact Fatigue of a Rail Steel*, Wear, 260, 2006, p. 523-537

[10] X. J. Zhao, et al., *Effects of Decarburization on the Wear Resistance and Damage Mechanisms of Rail Steels Subject to Contact Fatigue*, Wear, 364-365, 2016, p. 130-143

[11] E. Magel, *Validation of Electromagnetic Walking Stick Rail Surface Crack Measuring Systems*, DOT/FRA/ORD-16/23 Report, July 2016

[12] J. E. Garnham, C. L. Davis, *The Role of Deformed Rail Microstructure on Rolling Contact Fatigue Initiation*, Wear, 265, 2008, p. 1363-1372

[13] J. E. Garnham, C. L. Davis, *Very Early Stage Rolling Contact Fatigue Crack Growth in Pearlitic Rail Steels*, Wear, 271, 2011, p. 100-112

[14] D. Szablewski, *Quantifying Rail Surface Damage*, Wheel/Rail Interface (WRI) Conference, Heavy Haul Seminar, Montreal, Canada, 2017

[15] D. Szablewski, *Quantifying RCF in Rails: Methods, Practice, Outcomes*, International Collaborative Research Initiative (ICRI) Conference, Vancouver, Canada, 2017

[16] K. Oldknow, *Wheel-Rail Interaction Fundamentals*, Wheel/Rail Interface (WRI) Conference, Principles Course, Montreal, Canada, 2017